

# t-Channel Approach to Reggeon Interactions in QCD

**R. Kirschner**<sup>1</sup>

*Institut für Theoretische Physik, Universität Leipzig,  
D-04109 Leipzig, Germany*

## Abstract

Starting from the multi-Regge effective action for high-energy scattering in QCD a  $t$ -channel approach can be developed which is similar to the approach by White based on general Regge arguments. The BFKL kernel of reggeized gluon interaction, contributions to the  $2 \rightarrow 4$  reggeized gluon vertex function and the one-loop correction to the BFKL kernel are considered. The conditions are discussed under which this approach can provide a simple estimate of the next-to-leading logarithmic corrections to the BFKL perturbative pomeron intercept.

---

<sup>1</sup>*supported by Deutsche Forschungsgemeinschaft*

# 1 Introduction

Together with the progress in the experiments at HERA on deep-inelastic scattering at small  $x$  [1] the ideas and the results about the perturbative Regge asymptotics became popular. Long-standing results about the perturbative pomeron [2] [3] have found here a successful phenomenological application. Quite some effort has been applied in recent years to work out the corrections to the leading log results and also the predictions about distributions in the hadronic final state of small- $x$  deep-inelastic scattering.

We consider the part of the Regge region where the typical transverse momenta are large compared to the hadronic scale. It is natural and extremely useful to rewrite the leading perturbative contributions in this region in terms of the exchange of reggeized gluons, which interact among each other [2] [3] [4] [5] [6] [7].

A particular useful formulation is provided by the multi-Regge effective action [8] [9] [10], which can be obtained directly from the original QCD action by integration over modes of the fields, corresponding to momenta outside the kinematical range of scattering and exchanged gluons and quarks. Here we shall not be concerned with the case of quark exchange.

In this paper we discuss the relations of the multi-Regge effective action to a reggeon approach [11] [12] which reproduces the leading log reggeon interaction (BFKL kernel) and claims to predict some part of the higher loop corrections. The approach is based on an understanding about the connection between general Regge concepts to the perturbative and non-perturbative properties of non-abelian gauge theories developed by White in [6] (and references therein). The essential ingredients of the reconstruction procedure are signature-odd reggeons, related to the exchanged gluons, and their triple vertex, characterized by the non-sense zero behaviour:

$$\begin{aligned} \Gamma_{1,2}(\kappa, \kappa_1, \kappa_2) &= g(\omega - \alpha'|\kappa_1|^2 - \alpha'|\kappa_2|^2) \\ &\sim (|\kappa|^2 - |\kappa_1|^2 - |\kappa_2|^2) \quad \text{for } \omega = \alpha'|\kappa|^2, \\ &\sim |\kappa|^2 \quad \text{for } \kappa_{1,2} \rightarrow 0. \end{aligned} \tag{1.1}$$

$\alpha'$  is the slope of the Regge trajectory, which is taken to zero at the end.  $\omega = \alpha'|\kappa|^2$  is the position of the pole in the  $\omega$ -plane (here  $\omega + 1$  is the angular momentum) of the incoming reggeon propagator. Remarkably, those reggeons are colour singlets and the vertex has a trivial gauge-group structure.

Transitions of  $m$  to  $n$  reggeons in the  $t$ -channel are constructed step by step starting with the vertex (1.1) and applying a condition related to the Ward identities of the gauge theory:

$n \rightarrow m$  reggeon Green function vanish together with the transverse momentum of any in- or outgoing reggeon. Higher vertices are introduced additionally to (1.1) in order to obey this condition.

The property of vanishing at vanishing transverse momenta and its relation to gauge invariance has been noticed also in [13].

We point out that the triple vertex of exchanged gluons, emerging in the effective action as the induced vertex from the integration over heavy modes, has features close to the ones

of (1.1). Unlike White's reggeon vertex it carries the gauge-group structure of the ordinary triple-gluon vertex and depends on longitudinal momenta. We explain how this vertex can be used to reproduce the leading log results about the gluon reggeization and the (BFKL) interaction kernel in a t-channel approach close to [11]. The leading contribution to the  $2 \rightarrow 4$  QCD reggeon vertex has been constructed by Bartels [14]. There the transition kernels  $K_{2 \rightarrow n}$ , ( $n = 2, 3, 4$ ) obtained earlier [4] are the essential building blocks. We obtain these transition kernel in two ways from the multi-Regge effective action: From the effective scattering and production vertices (s-channel approach) and from the triple vertex of exchanged gluons (t-channel approach).

We discuss in detail the conditions on the gauge group state and the longitudinal momenta of the  $t$ -channel intermediate state under which the triple vertex of exchanged gluons can result in the  $\mathcal{O}(g^4)$  kernel proposed in [11] as the next-to-leading log correction to the QCD reggeon interaction (BFKL) kernel. From this it becomes clear in which sense the results of [11] [12] can approximate the full next-to-leading QCD calculations, some part of which has been done already [15], and whether the  $t$ -channel reggeon approach can become a tool to estimate higher order terms. In particular we point out a factor which is necessary to estimate the correction by using this  $\mathcal{O}(g^4)$  kernel.

Finally we outline our method of calculating the eigenvalue of the  $\mathcal{O}(g^4)$  kernel. The result is known and a method of calculation has been described in a recent paper [12]. That calculation is based on advanced methods [16]. Our approach is just a sequence of simple steps like the decomposition into partial fractions and the representation of cut-off regularization by complex contour integrals.

## 2 The triple vertex of exchanged gluons

The leading contribution to scattering processes in the perturbative Regge region which obey the multi-Regge kinematics in all sub-energy channels is described by the following effective action (restricted to gluons only):

$$\begin{aligned}
\mathcal{L} &= \mathcal{L}_{kin} + \mathcal{L}_s + \mathcal{L}_p + \mathcal{L}_t, \\
\mathcal{L}_{kin} &= -\frac{1}{2}(\partial^* \phi^a) \square (\partial \phi^{a*}) - 2\mathcal{A}_+^a \partial \partial^* \mathcal{A}_-^a, \\
\mathcal{L}_s &= -\frac{ig}{2}(\partial \phi^* T^a \overset{\leftrightarrow}{\partial}_- \partial^* \phi) \mathcal{A}_+^a + \frac{ig}{2}(\partial^* \phi^*) T^a \overset{\leftrightarrow}{\partial}_+ \partial \phi) \mathcal{A}_-^a, \\
\mathcal{L}_p &= g\phi^a(\partial \mathcal{A}_- T^a \partial^* \mathcal{A}_+) + g\phi^{a*}(\partial^* \mathcal{A}_- T^a \partial \mathcal{A}_+), \\
\mathcal{L}_t &= \frac{ig}{2}\partial \partial^* \mathcal{A}_-^a(\partial_+^{-1} \mathcal{A}_+ T^a \mathcal{A}_+) + \frac{ig}{2}\partial \partial^* \mathcal{A}_+^a(\partial_-^{-1} \mathcal{A}_- T^a \mathcal{A}_-)
\end{aligned} \tag{2.1}$$

We use the notations as in [9]. Four-vectors are decomposed into the two-dimensional components parallel (longitudinal) and orthogonal (transverse) to the plane determined by the (light-like) momentum vectors  $p_A, p_B$  of the incoming particles. The longitudinal component is parametrized by the light-cone coordinates and the transverse component

is represented by the corresponding complex number.

$$\begin{aligned} k_{\pm} &= k_0 \pm k_3, \kappa = k^1 + ik^2, \kappa^* = k^1 - ik^2, \\ x_{\pm} &= x_0 \pm x_3, x = x^1 + ix^2, x^* = x^1 - ix^2, \\ \partial_{\pm} &= \frac{1}{2}(\partial_0 \pm \partial_3), \partial = \frac{1}{2}(\partial_1 - i\partial_2), \partial^* = (\partial)^*. \end{aligned} \quad (2.2)$$

Further we use the abbreviation

$$(AT^a B) = -if^{abc} A^b B^c. \quad (2.3)$$

The complex scalar field  $\phi(x)$  represents the scattering gluons with their two helicity states. Correspondingly the momentum modes are restricted to the range close to mass shell.

$$\phi : |k_+ k_- - |\kappa|^2| \ll q_0^2. \quad (2.4)$$

$\mathcal{A}_{\pm}$  represent the exchanged gluons going from scattering particles with large  $k_{\mp}$  to scattering particles with large  $k_{\pm}$ . Their momentum modes are restricted to the range

$$\mathcal{A}_{\pm} : |k_+ k_-| \ll |\kappa|^2 \sim q_0^2. \quad (2.5)$$

Their propagator depends only on transverse momenta, as follows formally from (2.1), if the longitudinal momenta between which they are exchanged are ordered as described. According to (2.5) we have to adopt additionally that their propagator vanishes, if this longitudinal momentum ordering is violated.

Both  $\phi^a(x)$  and  $\mathcal{A}_{\pm}^a$  are directly related to the original gauge potential  $A_{\mu}^a$ . The restrictions on the momentum modes have been used extensively in deriving (2.1), in particular the modes with  $|k_+ k_-| \gg |\kappa|^2$  have been integrated out. The restrictions have to be imposed as additional conditions when constructing the leading log amplitudes from (2.1). When one relaxes the condition (2.4) on  $\phi$  one can disregard the triple interaction of exchanged gluons  $\mathcal{L}_t$  and the cut-off  $q_0$  does never appear.

The vertices in  $\mathcal{L}_p$ ,  $\mathcal{L}_s$  and  $\mathcal{L}_t$  are represented by graphs as in Fig. 1. Here (unlike in [9]) the dotted lines represent the scattering gluons  $\phi$  and the full lines the exchanged gluons  $\mathcal{A}_{\pm}$ . The  $t$ -channel is drawn in the horizontal direction. Scattering particles on the left (right) side carry large  $k_-(k_+)$ .

The exchanged gluons  $\mathcal{A}_{\pm}$  have features reminiscent to reggeons. One such feature is their orientation ( $\pm$ ) related to the longitudinal momentum ordering. The important point for this paper is the observation that their triple vertices  $\mathcal{L}_t$  have a transverse momentum dependence close to the non-sense zero structure (1.1) of the triple odd-signature reggeon vertex [6] [11]. For the vertex  $\mathcal{A}_- \rightarrow \mathcal{A}_+ \mathcal{A}_+$ , Fig. 1c, we have in the momentum representation

$$igf^{abc} \frac{|\kappa_1 + \kappa_2|^2}{k_{2+}}. \quad (2.6)$$

Notice that due to the longitudinal momentum ordering  $k_{2+} \approx -k_{1+}$  and within this accuracy the vertex is symmetric under exchanging  $(b, k_2) \leftrightarrow (c, k_1)$ . The vertex changes an odd-signature state (single exchanged gluon) into an even-signature state.

It is well known that the exchanged gluons reggeize. We repeat the corresponding discussion here in order to emphasize the role of the vertex  $\mathcal{L}_t$ <sup>2</sup> in comparison with the role of the effective vertex of gluon production  $\mathcal{L}_p$ .

Consider a state in the t-channel of one or two gluons corresponding to the adjoint representation. The leading log contributions to the amplitude with this exchange channel is determined by the graphs of Fig. 2 iterated in the *t*-channel direction. Iterating the box graph Fig. 2a only, constructed with the effective production vertices, one obtains the full contribution, if one removes the cut-off  $q_0$  in (2.2),  $q_0 \rightarrow \infty$ . More precisely, the sum of ladder graphs built with the effective vertex and with reggeized gluons in the *t*-channel results in a single reggeized gluon exchange (bootstrap).

Consider for arbitrary  $q_0$  the loop integral corresponding to Fig. 2b,

$$\frac{g^2 N}{2(2\pi)^3} \int \frac{dk_+ dk_-}{k_+ k_-} \int \frac{d^2 \kappa' |\kappa'|^4}{|\kappa'|^2 |\kappa - \kappa'|^2}. \quad (2.7)$$

We specify below the regularization necessary to give the transverse momentum integral a meaning. It is proportional to the deviation  $-g^2 N \alpha(\kappa)$  of the gluon trajectory from the angular momentum value  $j = 1$ .

$$\alpha(\kappa) = \frac{1}{2(2\pi)^3} \int \frac{d^2 \kappa' |\kappa'|^2}{|\kappa'|^2 |\kappa - \kappa'|^2}. \quad (2.8)$$

To understand the longitudinal momentum integral we restore the heavy-mode intermediate state [9] from which the triple vertex of exchanged gluons  $\mathcal{L}_t$  emerged. The heavy line in Fig. 3b represents the virtual gluon modes with

$$|k_+ k_- - |\kappa|^2| \gg q_0^2. \quad (2.9)$$

This step is similar to the way one understands reggeon diagrams of the form Fig. 3a. There reggeons can be replaced by scattering amplitudes in the Regge asymptotics as in Fig. 3c. Then the longitudinal momentum integration can be performed easily by using the analytic properties of the amplitudes  $A$  and  $B$  and substituting their dispersion integrals. Because of the cut-off condition (2.9) on the heavy modes the virtual gluon exchange in Fig. 3b does not correspond to  $A$  and  $B$  with normal analytic properties. Such properties hold, if we add Fig. 2 a,c,d. This is the way how in the presence of the cut-off  $q_0$  one arrives at the box graph including both the modes close and away from mass shell and obtains reggeization of the exchanged gluon. The dependence of the longitudinal momentum integral on the transverse momenta in the loop can be disregarded in the leading log approximation. We obtain the result for the sum of Fig. 2 by replacing in (2.7) the longitudinal momentum integral as

$$\int \frac{dk_+ dk_-}{k_+ k_-} \rightarrow \int \frac{s dk_+ dk_-}{[(p_A - k_0)^2 + i\epsilon][(p_B + k_0)^2 + i\epsilon]} \sim \ln \frac{s}{q_0^2} \quad (2.10)$$

---

<sup>2</sup>The role of this vertex in reggeization was clear to the authors of [9], but the papers contain only short comments.

$k_0$  is the four-vector with the longitudinal momenta  $k_+, k_-$  and the transverse momenta replaced by  $q_0$ .

Generalizing this observation we conclude that graphs with triple vertices of exchanged gluons can be regarded as reggeon diagrams, in particular for doing the longitudinal momentum integrals, if one adds appropriate contributions with with s-channel gluons close to mass shell.

### 3 The leading reggeon interaction

We consider the exchange of two gluons in the gauge group singlet channel and their interaction. The BFKL [2] kernel of reggeized gluon interaction is usually obtained by contracting two effective vertices of gluon production  $\mathcal{L}_p$  and including the gluon reggeization. Alternatively it can be obtained from the triple vertex of exchanged gluons ( $\mathcal{L}_t$ ) by interpreting the longitudinal momentum integration in the way appropriate to reggeon diagrams. This is the way how the derivation of the BFKL interaction kernel proposed in [11] fits in the framework of the QCD multi-Regge effective action.

The kernel is obtained as the contribution from the intermediate state in the  $t$ -channel with 3 exchanged gluons. The transition from 2 to 3 exchanged gluons is given by the graphs in Fig. 4 and by squaring we obtain the graphs Fig. 5. In the gauge group singlet channel all these graphs Fig. 5 give rise to the same gauge group factor. Also the longitudinal momentum integrals are the same up to signs. In fact the graphs contribute to the  $2 \rightarrow 2$  reggeon Green function  $f$  in the scattering amplitude Fig. 6. Therefore it is correct to evaluate the longitudinal momentum integrals as above including at this step implicitely contributions with intermediate scattering gluons close to mass shell. As contributions to the amplitude Fig. 6 the longitudinal momentum integral for each of the graphs Fig. 5 results in the same factor  $\sim \ln \frac{s}{q_0^2}$  in the leading log approximation.

The transverse momentum factors of the graphs give in the sum

$$\frac{|\kappa_1|^2 |\kappa'_2|^2}{|\kappa_1 - \kappa'_1|^2} + \frac{|\kappa_2|^2 |\kappa'_1|^2}{|\kappa_1 - \kappa'_1|^2} - |\kappa_2|^2 \alpha(\kappa_1) \delta(\kappa_2 - \kappa'_2) - |\kappa_1|^2 \alpha(\kappa_2) \delta(\kappa_1 - \kappa'_1), \quad (3.1)$$

where the terms are ordered as the graphs in Fig. 5 and the delta-function of momentum conservation  $\kappa_1 + \kappa_2 = \kappa'_1 + \kappa'_2$  has been omitted.  $\alpha(\kappa)$  denotes the transverse momentum integral in (2.8) which determines the gluon trajectory. The minus sign in front of the last two terms arises from the longitudinal momenta in the vertices (2.6). The weight  $\frac{1}{2}$  in the trajectory integral  $\alpha(k)$  is due to Bose symmetry.

By evaluating the longitudinal intergral as in reggeon diagrams we include contributions beyond the ones originally represented by the graphs with the triple vertices of exchanged gluons (2.6). Following this line we cannot be sure that we recover all leading contributions. Instead of going back to the effective action and analyzing all contributions one can use at this point the property of reggeon Green functions to vanish with vanishing transverse momenta. Whereas the last two terms in (3.1) satisfy this condition trivially

the first two terms do not. Obviously the term

$$-|\kappa_1 + \kappa_2|^2 \quad (3.2)$$

has to be added to (3.1). The missing contribution corresponds to a new quartic vertex of exchanged gluons ( $\mathcal{A}_-\mathcal{A}_-\mathcal{A}_+\mathcal{A}_+$ ) Fig. 7 having the same gauge group factor and longitudinal momentum integrals as the graphs Fig. 5 but the transverse momentum structure (3.2). The sum of (3.1) and (3.2) is the known BFKL interaction kernel. Its connected part (omitting the last two terms in (3.1) ) is denoted by  $K_{2 \rightarrow 2}$  according to [4],

$$\begin{aligned} K_{2 \rightarrow 2}(\kappa_1, \kappa_2; \kappa'_1, \kappa'_2) &= -|\kappa_1 + \kappa_2|^2 + \frac{|\kappa_1|^2 |\kappa'_2|^2 + |\kappa_2|^2 |\kappa'_1|^2}{|\kappa_1 - \kappa'_1|^2} \\ &= \frac{\kappa_1 \kappa'^*_1 \kappa^*_2 \kappa'_2 + \text{c.c.}}{|\kappa_1 - \kappa'_1|^2}. \end{aligned} \quad (3.3)$$

The second form correspond to the transverse momentum part of the graph Fig. 8a, obtained by contracting two effective production vertices  $\mathcal{L}_p$ , and the two terms in the numerator correspond to the two helicities of the s-channel gluon.

The transition kernels  $K_{2 \rightarrow 3}, K_{2 \rightarrow 4}$ , which are a result of the s-channel unitarity analysis in [4] and which are building blocks of the  $2 \rightarrow 4$  reggeon Green function [11], can be most easily obtained as the transverse momentum factors of the graphs Fig. 9a and 10a, correspondingly. With the effective vertices of scattering  $\mathcal{L}_s$  and production  $\mathcal{L}_p$  we obtain

$$\begin{aligned} K_{2 \rightarrow 3}(\kappa_1, \kappa_2; \kappa'_1, \kappa'_2, \kappa'_3) &= \frac{\kappa_1 \kappa'^*_1 \kappa^*_2 \kappa'_3}{(\kappa_1 - \kappa'_1)^* (\kappa_2 - \kappa'_3)} + \text{c.c.} \quad , \\ K_{2 \rightarrow 4}(\kappa_1, \kappa_2; \kappa'_1, \kappa'_2, \kappa'_3, \kappa'_4) &= \frac{\kappa_1 \kappa'^*_1 \kappa^*_2 \kappa'_4}{(\kappa_1 - \kappa'_1)^* (\kappa_2 - \kappa'_4)} + \text{c.c.} \quad . \end{aligned} \quad (3.4)$$

In [14] all t-channel gauge group and signature states of the two incoming and the four outgoing reggeized gluons in the  $2 \rightarrow 4$  reggeon Green function are considered. Clearly this variety of cases cannot be reconstructed by the vertex (1.1) and therefore the reggeon Green functions in [11] and [14] are not compatible. However the following discussion shows, that also here a t-channel approach works. We rederive  $K_{2 \rightarrow 3}, K_{2 \rightarrow 4}$ , using  $K_{2 \rightarrow 2}$  (3.3), which we have already obtained by t-channel analysis, and the triple vertex of exchanged gluons (2.6). We disregard now the gauge group structure and concentrate on the transverse momentum factors corresponding to the graphs only.

Consider the graphs in Fig. 11. They are obtained by contracting the elementary splitting  $2 \rightarrow 3$ , Fig. 4, with a pairwise interaction of the 3 exchanged gluons via  $K_{2 \rightarrow 2}$ . The right-hand side is obtained by inserting  $K_{2 \rightarrow 2}$  as the sum of graphs Fig. 8b, where for convenience we write the minus sign associated above with the quartic vertex Fig. 7 (3.2) explicitly in front of the graph. Further we have contracted those lines the propagators of which are cancelled by factors in the adjacent vertices. Representing now merely transverse momentum expressions, the meaning of the graphs, in particular of the vertex  $(\mathcal{A}_-\mathcal{A}_+\mathcal{A}_+\mathcal{A}_+)$  emerging by this contraction, is obvious.

Consider Fig. 12, where now the incoming two gluons interact via  $K_{2 \rightarrow 2}$  and the splitting Fig. 4 appears afterwards. Comparing the resulting graphs we observe, that the difference of Fig. 11 and Fig. 12 is  $2 K_{2 \rightarrow 3}$ , where  $K_{2 \rightarrow 3}$  is given by the sum of graphs in Fig. 9b or by the expression (with the terms in the same order as the graphs)

$$K_{2 \rightarrow 3}(\kappa_1, \kappa_2; \kappa'_1, \kappa'_2, \kappa'_3) = -|\kappa_1 + \kappa_2|^2 + \frac{|\kappa'_1 + \kappa'_2|^2 |\kappa_2|^2}{|\kappa_2 - \kappa'_3|^2} + \frac{|\kappa'_2 + \kappa'_3|^2 |\kappa_1|^2}{|\kappa_1 - \kappa'_1|^2} - \frac{|\kappa_1|^2 |\kappa_2|^2 |\kappa'_2|^2}{|\kappa_2 - \kappa'_3|^2 |\kappa_1 - \kappa'_1|^2}. \quad (3.5)$$

We have seen that Bartels' transition kernel  $K_{2 \rightarrow 3}$  is proportional to the connected part of the convolution of the elementary splitting  $2 \rightarrow 3$  with the pairwise interaction via  $K_{2 \rightarrow 2}$  modulo  $K_{2 \rightarrow 2}$  convoluted with subsequent  $2 \rightarrow 2$  elementary splitting.

The analogous relation holds for the transition kernel  $K_{2 \rightarrow 4}$ , only the interaction  $K_{2 \rightarrow 2}$  is to be replaced by the transition of pairs the exchanged gluons into three gluons via  $K_{2 \rightarrow 3}$ . Indeed, the difference of Fig. 13 and Fig. 14 is  $3 K_{2 \rightarrow 4}$ , where  $K_{2 \rightarrow 4}$  is represented by the sum of graphs in Fig. 10b or by the sum of terms corresponding to these 4 graphs,

$$K_{2 \rightarrow 4}(\kappa_1, \kappa_2; \kappa'_1, \kappa'_2, \kappa'_3, \kappa'_4) = -|\kappa_1 + \kappa_2|^2 + \frac{|\kappa'_1 + \kappa'_2 + \kappa'_3|^2 |\kappa_2|^2}{|\kappa_2 - \kappa'_4|^2} + \frac{|\kappa'_2 + \kappa'_3 + \kappa'_4|^2 |\kappa_1|^2}{|\kappa_1 - \kappa'_1|^2} - \frac{|\kappa_1|^2 |\kappa_2|^2 |\kappa'_2 + \kappa'_3|^2}{|\kappa_2 - \kappa'_4|^2 |\kappa_1 - \kappa'_1|^2}. \quad (3.6)$$

The coincidence of the expressions (3.4), (3.5) for  $K_{2 \rightarrow 3}$  and (3.4), (3.6) for  $K_{2 \rightarrow 4}$  can be checked by straightforward calculations. We recommend to consider the limiting cases of vanishing and large momentum transfer  $\kappa_1 + \kappa_2$ .

## 4 The one-loop reggeon interaction

The one-loop corrections arise from the s-channel configurations, where pairs of particles do not have a large sub-energy and their longitudinal momenta violate the multi-Regge strong ordering. It is not obvious at all that the procedure, where longitudinal momentum integrals are treated as in reggeon diagrams, can give some reasonable result here. In the  $t$ -channel approach the one-loop correction to the BFKL kernel arises from the contribution to the two-gluon exchange (Fig. 6) by 4 gluons in the  $t$ -channel intermediate state. Analogous to the case of 3 intermediate gluons above the integration over the longitudinal momenta has to be considered for the graphs inserted in the amplitude Fig. 6. But now only one of the two loop integrals with the additional intermediate gluons gives a contribution  $\sim \ln s$ . The leading log arguments which allowed above to separate the longitudinal from the transverse momentum intergrals are not applicable here.

Our point is to formulate assumptions under which such a separation would hold and under which the formula obtained in [11] would make sense. Unavoidably this takes to introduce a scale, which cannot be fixed within the framework of the approach.

At this place one might feel disappointed and prefer to wait for the full QCD next-to-leading calculation. Nevertheless it may be worthwhile to look for a scheme allowing eventually to obtain a simple estimate of the higher loop corrections.

We discuss schematically the integration over the longitudinal momenta. Consider the contributions to the amplitude Fig. 15. Treating the exchanged gluons as reggeons the longitudinal momentum integrals over  $k_{2+}, k_{1+}$  can be done by taking residues (under the dispersion integrals for the amplitudes  $A, B$ ) at appropriate poles. We arrive in the second case, Fig. 15 b, at

$$\int_{q_0}^{\sqrt{s}} \frac{dk_{1-} dk_{2-}}{k_{1-} k_{2-}} \theta(k_{1-} - k_{2-}) = \int_0^Y dy_{1-} dy_{2-} \theta(y_{1-} - y_{2-}) = \frac{1}{2} Y^2. \quad (4.1)$$

We use the notations  $y_- = \ln \frac{k_-}{q_0}$ ,  $Y = \frac{1}{2} \ln \frac{s}{q_0^2}$ . In the first case, Fig. 15 a, we encounter contradicting ordering conditions. The result is complicated, depending in particular on the transverse momenta.

In order to proceed without working out the details, one has to assume that these integrals can be approximated nevertheless by logarithmic integrals in  $k_{1-}, k_{2-}$  with relaxed ordering conditions:

$$\int_0^Y dy_{1-} dy_{2-} \theta(y_{1-} - y_{2-} + \eta) \theta(y_{2-} - y_{1-} + \eta) = Y 2\eta. \quad (4.2)$$

In any case, at large  $Y$ , the result can be written in this form, but then  $\eta$  is a function depending on transverse momenta and this dependence is different for each graph Fig. 17.

One can write  $\eta = \ln \frac{q_1}{q_0}$  and interpret  $q_0$  as the typical transverse momentum and  $q_1$  as characterizing the width of the transverse momentum range.

We consider the splitting of two exchanged gluons in the gauge group singlet state into 4 gluons, Fig. 16. The gauge group state of the 4 gluons can be characterized by the quantum numbers in a two-gluon sub-channel as in [14]. One can choose the two gluons the  $k_+$  of which enters the expression. We give them the numbers 2 and 3. Only the state symmetric in the gauge group indices of these two gluons contributes as an intermediate state to the kernel. The antisymmetric (adjoint representation) state contributes to reggeization and will be accounted for elsewhere. The longitudinal momenta of these two gluons are close to each other,

$$|\ln \frac{k_{2+}}{k_{1+}}| < \eta, \quad |\ln \frac{k_{2-}}{k_{1-}}| < \eta. \quad (4.3)$$

We obtain the correction to the kernel by contracting the  $2 \rightarrow 4$  graphs Fig. 16 with corresponding  $4 \rightarrow 2$  graphs. The longitudinal momentum integrals, considered as contributions to the amplitude Fig. 6 and approximated as in (4.2), are universal in all terms. Also the gauge group matrices give rise to an universal factor proportional to

$$(\mathbf{tr}(T^a T^b T^a T^b) + \mathbf{tr}(T^a T^b T^b T^a)) / (N^2 - 1). \quad (4.4)$$

After the separation of the longitudinal momentum and the gauge group structures the graphs can be considered as representing transverse momentum expressions only. As in the previous section we contract the intermediate lines, e.g. in Fig. 16a and 16b, the propagators of which are cancelled by factors in the vertices. We arrive at the graphs in Fig. 17. As a remainder from the longitudinal momenta the graphs in the second line enter with a minus sign. In front of the loop integrals the following Bose symmetry factors appear:  $\frac{1}{3!}$  in the first two graphs,  $(\frac{1}{2!})^2$  in the third graph and  $\frac{1}{2!}$  in the remaining graphs besides of the last one. Since the expression can be read off easily from the graphs we shall not write it here. We check that the resulting one-loop correction to the reggeon Green function obeys the condition of vanishing with any of the transverse momenta. No new vertex and no loop correction in the existing vertices has to be introduced.

Summarizing, we have seen that in order to reproduce the result of [11] the longitudinal momentum integration has to be approximated and the gauge group intermediate state has to be restricted. Therefore the one-loop correction enters the reggeon interaction kernel with the factor

$$\eta \frac{3}{2} N^2. \quad (4.5)$$

It will be interesting to compare with the full QCD calculation and to ask whether it can be represented by transverse momentum expressions corresponding to the graphs Fig. 17 with each term modified by a function  $\eta(\kappa_1\dots)$  inserted in the integrand, weakly depending on the transverse momenta and different from term to term.

## 5 Calculating the eigenvalues

Here we outline our method of the eigenvalue calculation for the one-loop interaction kernel given by the graphs Fig. 17 in the forward limit,  $\kappa_2 = -\kappa_1 = \kappa$ ,  $\kappa'_2 = -\kappa'_1 = \kappa'$ .

$$\int \frac{d^2\kappa'}{|\kappa'|^4} K^{(4)}(\kappa, \kappa') f_{n,\nu}(\kappa') = \Omega^{(4)}(n, \nu) f_{n,\nu}(\kappa). \quad (5.1)$$

The eigenfunctions are the same as for the lowest order kernel [13],

$$f_{n,\nu}(\kappa) = |\kappa^2|^{1/2+i\nu} \left( \frac{\kappa}{|\kappa|} \right)^n \quad (5.2)$$

( $-\infty < \nu < \infty$ ,  $n$  integer), and the one-loop kernel at vanishing momentum transfer is given by

$$\begin{aligned} K^{(4)}(\kappa, \kappa') = & (2\pi)^3 |\kappa|^6 \left( \frac{1}{3} J_2(\kappa) + \frac{1}{4} (J_1(\kappa))^2 \right) \delta(\kappa - \kappa') \\ & - |\kappa - \kappa'|^{-2} \left( 2|\kappa|^4 J_1(\kappa) |\kappa'|^2 + 2|\kappa|^2 J_1(\kappa') |\kappa'|^4 \right) \\ & + 2J_1(\kappa - \kappa') |\kappa|^2 |\kappa'|^2 + 2|\kappa|^4 |\kappa'|^4 I(\kappa, \kappa') \\ & + (\kappa' \leftrightarrow -\kappa') \end{aligned} \quad (5.3)$$

The terms are ordered in the same way as the graphs in Fig. 17. By adding the corresponding expression with the opposite sign in front of  $\kappa'$  one projects on the positive signature channel. The notation for the loop integrals are the same as in [11],

$$\begin{aligned} J_1(\kappa) &= (2\pi)^{-3} \int d^2\kappa' |\kappa'|^{-2} |\kappa - \kappa'|^{-2} = |\kappa|^{-2} \alpha(\kappa), \\ J_2(\kappa) &= (2\pi)^{-3} \int d^2\kappa' |\kappa - \kappa'|^{-2} J_1(\kappa'), \\ I(\kappa, \kappa') &= (2\pi)^{-3} \int d^2\kappa'' |\kappa''(\kappa'' - \kappa)(\kappa'' + \kappa')(\kappa'' - \kappa + \kappa')|^{-2}. \end{aligned} \quad (5.4)$$

The integrands are moduli squared of rational expressions. The latter can be decomposed into simple fractions. This is the essential step in calculating the contribution of  $I(\kappa, \kappa')$  to the eigenvalue in our approach.

$$[\kappa''(\kappa'' - \kappa)(\kappa'' + \kappa')(\kappa'' - \kappa + \kappa')]^{-1} = \frac{1}{\kappa\kappa'} \left\{ \frac{1}{\kappa' - \kappa} \left( \frac{1}{\kappa''} - \frac{1}{\kappa'' - \kappa + \kappa'} \right) \right. \\ \left. + \frac{1}{\kappa' + \kappa} \left( \frac{1}{\kappa'' - \kappa} - \frac{1}{\kappa'' + \kappa'} \right) \right\} \quad (5.5)$$

In this way  $I(\kappa, \kappa')$  is decomposed into two parts,

$$\begin{aligned} &2|\kappa|^4 |\kappa'|^4 I(\kappa, \kappa') + (\kappa' \leftrightarrow -\kappa') = K_2^{(4)}(\kappa, \kappa') \\ &+ \frac{2}{(2\pi)^3} \int d^2\kappa'' \left| \frac{1}{\kappa''} - \frac{1}{\kappa'' - \kappa + \kappa'} \right|^2 |\kappa' - \kappa|^{-2} |\kappa|^2 |\kappa'|^2 + (\kappa' \leftrightarrow -\kappa'), \end{aligned} \quad (5.6)$$

where

$$K_2^{(4)}(\kappa, \kappa') = \frac{2}{(2\pi)^3} \int d^2\kappa'' \left( \frac{1}{\kappa''} - \frac{1}{\kappa'' - \kappa + \kappa'} \right) \left( \frac{1}{\kappa'' - \kappa} - \frac{1}{\kappa'' + \kappa'} \right)^* \\ \cdot (\kappa' - \kappa)^{-1} (\kappa' + \kappa)^{* -1} + \text{c.c.} \quad (5.7)$$

Because the integral in the second term of (5.6) is  $J_1(\kappa - \kappa')|\kappa - \kappa'|^2$ , this term coincides with the last of the remaining terms in  $K^{(4)}$  (5.3). It is natural to decompose the kernel,

$$K^{(4)} = K_1^{(4)} + K_2^{(4)}. \quad (5.8)$$

Moreover this decomposition is reasonable owing to the infrared divergence cancellation. The integral defining  $K_2^{(4)}$  and also the integral defining the action of  $K_2^{(4)}$  are free of divergencies.

It is not difficult to check that the divergencies in the terms of  $K_1^{(4)} \otimes f$  cancel against each other. If we want to calculate the eigenvalue of  $K_1^{(4)}$  term by term we have to introduce a regularization. Because the decomposition (5.6) related to the partial fractions works only in exactly 2 dimensions we avoid the dimensional regularization. In the complex planes of  $\kappa'$  and  $\kappa''$  we cut out small discs of radius  $\lambda$  around all singularities. We represent the step function imposing this cut-off by  $(\delta \rightarrow +0)$

$$\theta(|\kappa' - \kappa| - \lambda) = \frac{1}{2\pi i} \int_{-i\infty+\delta}^{i\infty+\delta} \frac{d\omega}{\omega} \left( \frac{|\kappa' - \kappa|^2}{\lambda^2} \right)^\omega. \quad (5.9)$$

With this representation the next steps of the calculation are close to the ones in dimensional regularization. In the Appendix we explain the calculation of  $J_1(\kappa)$  and of the eigenvalue of one term in  $K_1^{(4)}$ . The resulting eigenvalue is [11]

$$\begin{aligned}\Omega_1^{(4)}(n, \nu) &= \frac{2}{\pi}(1 + (-1)^n)(\chi(n, \nu))^2, \\ \chi(n, \nu) &= \psi(1) - \frac{1}{2}\psi\left(\frac{1}{2} + i\nu + \frac{|n|}{2}\right) - \frac{1}{2}\psi\left(\frac{1}{2} - i\nu + \frac{|n|}{2}\right).\end{aligned}\quad (5.10)$$

Now we turn to  $K_2^{(4)}$  (5.7). We calculate the intergral over  $\kappa''$  reducing it by shifts to  $J_1(\kappa) - J_1(\kappa')$ . This leads to the representation

$$\begin{aligned}(2\pi)^3 \int \frac{d^2\kappa'}{|\kappa'|^4} K_2^{(4)}(\kappa, \kappa') f_{n,\nu}(\kappa') &= -4\pi f_{n,\nu} \frac{d}{d\omega} J_\omega(n, \nu) |_{\omega=0}, \\ J_\omega(n, \nu) &= \int d^2y |y^2|^{-1/2+i\nu-\omega} \left(\frac{y}{|y|}\right)^n \left(\frac{1}{(y-1)(y+1)^*} + \text{c.c.}\right).\end{aligned}\quad (5.11)$$

We introduce polar coordinates,  $y = re^{i\phi}$ , and do the integral over  $\phi$  by taking residues in the complex plane of  $z = e^{i\phi}$ . In the intermedialte steps the  $r$  integral is divided into  $0 < r < 1$  and  $1 < r < \infty$ . Inversion in the second term leads to

$$J_\omega(n, \nu) = 2\pi(1 + (-1)^n) \int_0^1 \frac{dr}{r^2 + 1} r^{|n|} (r^{-2i\nu+2\omega} - r^{2i\nu-2\omega}).\quad (5.12)$$

This integral can now be expressed in terms of the incomplete beta function [17],

$$\beta(p) = \int_0^1 \frac{x^{p-1} dx}{x+1} = \frac{1}{2} \left(\psi\left(\frac{p+1}{2}\right) - \psi\left(\frac{p}{2}\right)\right).\quad (5.13)$$

We obtain finally

$$\Omega_2^{(4)}(n, \nu) = -\frac{1}{2\pi}(1 + (-1)^n) \left(\beta'\left(\frac{|n|+1}{2} + i\nu\right) + \text{c.c.}\right),\quad (5.14)$$

where the prime denotes the derivative of the function.

The discussion of the interesting properties of the result related to conformal symmetry and holomorphic factorization [18] [19] and the numerical evaluation of the leading eigenvalue has been given in [12]. We emphasize that as a result of our analysis the one-loop kernel  $K^{(4)}$  and therefore the eigenvalues  $\Omega^{(4)}$  enter multiplied by the factor (4.5).

## 6 Discussion

The multi-Regge effective action is a tool for investigating the Regge asymptotics. The leading logarithmic approximation to the high-energy asymptotics is reproduced easily by using the lowest order effective vertices of scattering and production. The lowest order effective action provides a starting point to study those corrections to the leading log

approximation, which are related to the multiple exchange of reggeized gluons and which are responsible for restoring unitarity in all sub-energy channels. Mostly this study has been approached from the point of view of  $s$ -channel intermediate states. Alternatively the point of view of  $t$ -channel intermediate states can be taken. It leads to an essentially different way for obtaining the leading log amplitudes and the unitarity corrections.

The gluons exchanged in the  $t$ -channel behave like signature-odd reggeons. This observation is confirmed in particular by the similarity of the triple vertex of exchanged gluons in the multi-Regge effective action to the triple vertex of signature-odd reggeons considered in [6] [11]. We have shown that starting from this vertex in the effective action a  $t$ -channel approach similar to the one in [11] works. The BFKL leading log interaction kernel of reggeized gluons and the transition kernels [4] [14], which are relevant for the unitarity corrections, have been reconstructed in this approach.

Graphs with the triple vertex of exchange gluons can be treated as reggeon diagrams, in particular the longitudinal momentum integrals can be interpreted in this way. This amounts to include implicitly contributions with scattering gluons in  $s$ -channel intermediate states.

There are more corrections to the leading log approximation besides of those which improve the unitarity properties. In the effective action such next-to-leading log corrections give rise to corrections to the effective vertices, to corrections to the trajectory and to new vertices [15] [10]. The corrected production vertices and the corrected trajectory result in the corrected BFKL kernel.

Starting from the effective action on the leading log level, in particular from the triple vertex of exchanged gluons, and applying the  $t$ -channel analysis following basically the one by White [11], we obtain an one-loop interaction kernel. Our discussion above shows to what extend this kernel can be a reasonable estimate of the full next-to-leading log correction to the BFKL kernel. In particular we point out a factor in front of this one-loop kernel involving a scale, which arises from approximating the longitudinal momentum integrals. We expect that the full next-to-leading log kernel has a similar structure with this rapidity factor replaced in each term by a function weakly depending on the transverse momenta.

The loop integrals encountered in the eigenvalue calculation can be done without major effort by using the simplicity of the integrands. They are moduli squared of rational expressions, which can be decomposed into simple fractions.

## Acknowledgements

The author is grateful to A.R. White for discussions and for hospitality at Argonne. He had also useful discussions with J. Bartels, L.N. Lipatov and L. Szymanowski. The financial support by Deutsche Forschungsgemeinschaft is gratefully acknowledged.

## Appendix

We calculate  $J_1(\kappa)$  (5.4) regularized as described (5.9).

$$\begin{aligned} (2\pi)^3 J_1(\kappa)|_{reg} &= \int \frac{d^2\kappa'}{|\kappa'|^2|\kappa - \kappa'|^2} \theta(|\kappa'| - \lambda) \theta(|\kappa' - \kappa| - \lambda) \\ &= \frac{1}{(2\pi i)^2} \int \frac{d\omega_0}{\omega_0} \frac{d\omega}{\omega} \lambda^{-2\omega_0-2\omega} \int \frac{d^2\kappa'}{|\kappa'|^{2-2\omega_0}|\kappa - \kappa'|^{2-2\omega}}. \end{aligned} \quad (6.15)$$

We do the integral over  $\kappa'$  and arrive at

$$\begin{aligned} &\frac{\pi}{(2\pi i)^2} \int \frac{d\omega_0}{\omega_0} \frac{d\omega}{\omega} \left( \frac{|\kappa|^2}{\lambda^2} \right)^{-\omega_0-\omega} \left( \frac{1}{\omega_0} + \frac{1}{\omega} \right) \\ &\frac{\Gamma(1 - \omega_0 - \omega)\Gamma(1 + \omega)\Gamma(1 + \omega_0)}{\Gamma(1 + \omega_0 + \omega)\Gamma(1 - \omega)\Gamma(1 - \omega_0)}. \end{aligned} \quad (6.16)$$

For  $|\kappa| > \lambda$  we obtain

$$\frac{\pi}{(2\pi i)} \int \frac{d\omega}{\omega^2} \left| \frac{\kappa^2}{\lambda^2} \right|^\omega = 2\pi \ln \left| \frac{\kappa^2}{\lambda^2} \right|. \quad (6.17)$$

We pick up one term out of  $K_1^{(4)} \otimes f_{n,\nu}$ :

$$\begin{aligned} &(2\pi)^3 \int d\kappa' J_1(\kappa - \kappa') |\kappa'|^{-2} |\kappa|^{-2} f_{n,\nu}(\kappa') \quad |_{reg} \\ &= \frac{1}{(2\pi i)^3} \int \frac{d\nu_0}{\nu_0} \frac{d\nu_1}{\nu_1} \frac{d\omega}{\omega} \lambda^{-2\nu_0-2\nu_1-2\omega} 2\pi \int \frac{d^2\kappa' \kappa'^n}{|\kappa'|^{2-2\nu_0-1-2i\nu} |\kappa - \kappa'|^{2-2\nu_1-2\omega}} \\ &= f_{n,\nu}(\kappa) \frac{2\pi^2}{2\pi i} \int \frac{d\omega}{\omega^3} \left( \frac{|\kappa|^2}{\lambda^2} \right)^\omega \frac{\Gamma(\frac{1}{2} + i\nu + \frac{|n|}{2})\Gamma(1 + \omega)\Gamma(\frac{1}{2} - i\nu + \frac{|n|}{2} - \omega)}{\Gamma(\frac{1}{2} + i\nu + \frac{|n|}{2} + \omega)\Gamma(1 - \omega)\Gamma(\frac{1}{2} - i\nu + \frac{|n|}{2})} \\ &= f_{n,\nu}(\kappa) 2\pi^2 \left\{ \frac{1}{2} \ln^2 \left| \frac{\kappa^2}{\lambda^2} \right| + \ln \left| \frac{\kappa^2}{\lambda^2} \right| 2\chi(n, \nu) + \frac{d}{d(i\nu)} \chi(n, \nu) + 2(\chi(n, \nu))^2 \right\}. \end{aligned} \quad (6.18)$$

We have used the notation as in (5.10).

## References

- [1] I. Abt et al., H1 Collaboration, Nucl. Phys. B407 (1993), 515;  
M. Derrick et al., Zeus Collaboration, Phys. Lett. 316B (1993) 412; Zeitschr. f. Phys. C59 (1993), 231.
- [2] V.S. Fadin, E.A. Kuraev and L.N. Lipatov, Phys. Lett. 60B(1975)50; ZhETF 71(1976)840; *ibid* 72(1977)377  
Y.Y. Balitski and L.N. Lipatov, Sov. J. Nucl. Phys. 28(1978) 882
- [3] H. Cheng and C.Y. Lo, Phys. Rev. D13 (1976), 1131 and D15 (1977), 2959.
- [4] J. Bartels, Nucl. Phys. B151 (1979), 293; *ibid*. B175(1980), 365.
- [5] J. Kwiecinski and M. Praszalowicz, Phys. Lett. B94(1980), 413.
- [6] A.R. White, Int. J. Mod. Phys. A6 (1990), 1859
- [7] L.N. Lipatov in "Perturbative QCD" A.H. Mueller ed., World Scientific 1989
- [8] L.N. Lipatov, Nucl. Phys. B365(1991)614
- [9] R. Kirschner, L.N. Lipatov and L. Szymanowski, Nucl. Phys. B425(1994), 579;  
Phys. Rev. D51(1995), 838.
- [10] L.N. Lipatov, "Gauge invariant effective action for high-energy processes in QCD",  
DESY preprint 1995
- [11] A. R. White, Phys. Lett. B339 (1994), 87;  
A. White and C. Coriano, Argonne preprint ANL-HEP-CP 94-79, to appear in the  
proceedings of Int. Symposium on Multiparticle Dynamics, Vietri sul Mare, Sept.  
1994
- [12] A. White and C. Coriano, Argonne preprints ANL-HEP-PR 94-84 and ANL-HEP-PR  
95-12
- [13] L.N. Lipatov, ZhETF 90 (1986), 536
- [14] J. Bartels, preprint DESY 91-074 (1991), unpublished; Zeitschr. f. Phys. C60(1993),  
471;  
J. Bartels and M. Wüsthoff, preprint DESY 94-016 (1994)
- [15] V.S. Fadin and L.N. Lipatov, Pisma ZhETF 46 (1989), 311; Yad. Fiz. 50 (1989),  
1141; Nucl. Phys. B406 (1993), 259.
- [16] G. Källen and J. Toll, J. Math. Phys. 6 (1965), 299.
- [17] I.S. Gradshteyn and I.M. Ryzhik, Tables of integrals, Nauka, Moscow 1971.

- [18] L.N. Lipatov, Phys. Lett 251B (1990) 284
- [19] R. Kirschner, Zeitschr. f. Phys. C65 (1995), 505.

## Figure captions

Fig. 1 Vertices of the effective action. a) Effective vertex of emission, b) effective vertex of scattering, c) triple vertex of exchanged gluons.

Fig. 2 Contributions to reggeization of exchanged gluons.

Fig. 3 Interpretation of the longitudinal momentum integral.

Fig. 4  $2 \rightarrow 3$  splitting of exchanged gluons.

Fig. 5 Contributions to the  $2 \rightarrow 2$  Green function of reggeized gluons.

Fig. 6 Contribution of the  $2 \rightarrow 2$  reggeon Green function to the scattering amplitude.

Fig. 7 Quartic vertex of exchanged gluons.

Fig. 8 The transition kernel  $2 \rightarrow 2$  in s-channel (a) and t-channel (b) representations.

Fig. 9 The transition kernel  $2 \rightarrow 3$  in s-channel (a) and t-channel (b) representations.

Fig. 10 The transition kernel  $2 \rightarrow 4$  in s-channel (a) and t-channel (b) representations.

Fig. 11 Contraction of the  $2 \rightarrow 3$  splitting with the  $K_{2 \rightarrow 2}$  interaction.

Fig. 12 Contraction of  $K_{2 \rightarrow 2}$  with the  $2 \rightarrow 3$  splitting.

Fig. 13 Contraction of the  $2 \rightarrow 3$  splitting with the transition kernel  $K_{2 \rightarrow 3}$ .

Fig. 14 Contraction of the transition kernel  $K_{2 \rightarrow 3}$  with the  $3 \rightarrow 4$  splitting.

Fig. 15 Contributions to the scattering amplitude.

Fig. 16 Graphs contributing to the  $2 \rightarrow 4$  splitting.

Fig. 17 Transverse momentum graphs for the one-loop correction to the  $2 \rightarrow 2$  reggeon Green function.

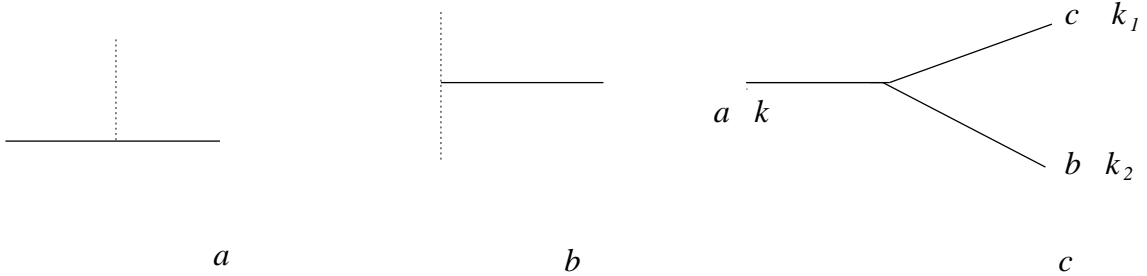


Figure 1: *Vertices of the effective action. a) Effective vertex of emission, b) effective vertex of scattering, c) triple vertex of exchanged gluons.*

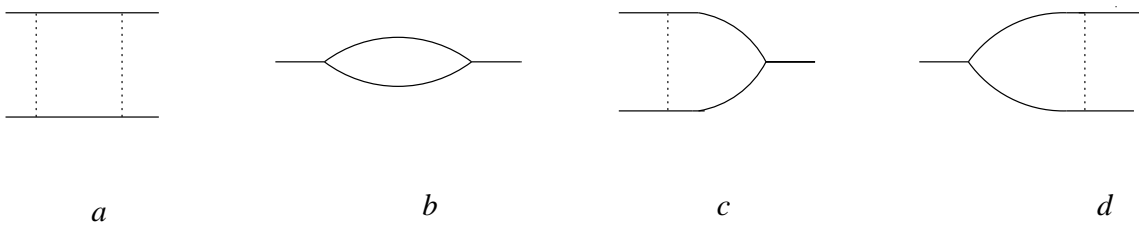


Figure 2: *Contributions to reggeization of exchanged gluons.*

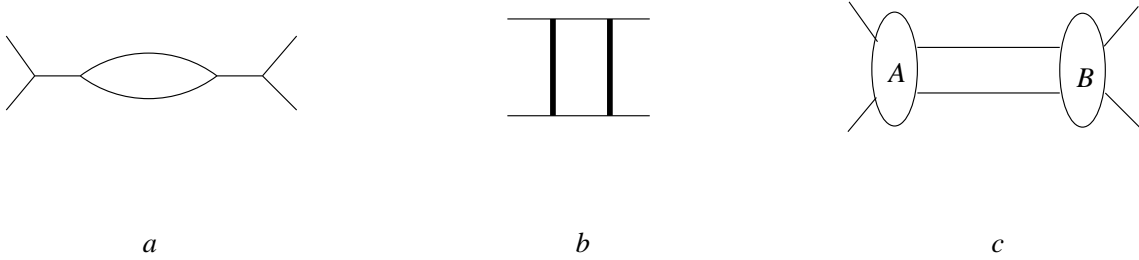


Figure 3: *Interpretation of the longitudinal momentum integral.*

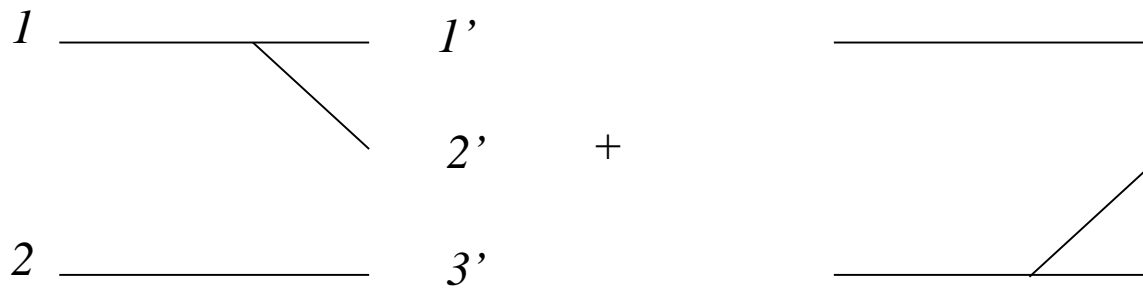


Figure 4:  $2 \rightarrow 3$  splitting of exchanged gluons.

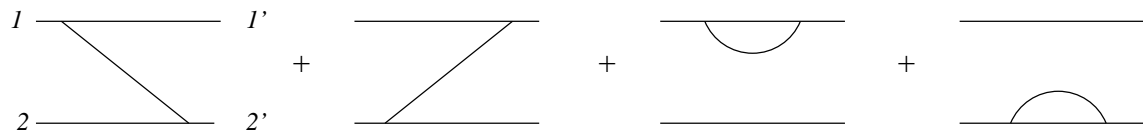


Figure 5: Contributions to the  $2 \rightarrow 2$  Green function of reggeized gluons.

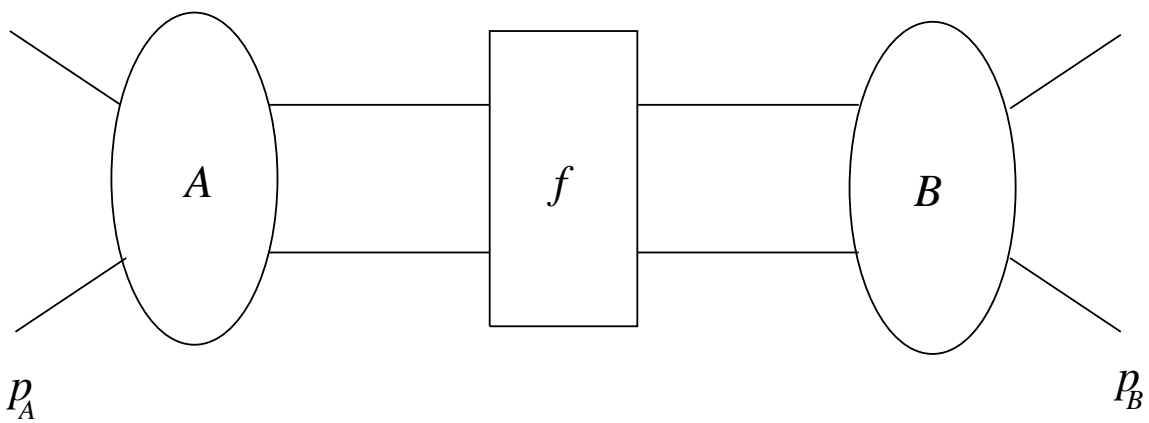


Figure 6: Contribution of the  $2 \rightarrow 2$  reggeon Green function to the scattering amplitude.

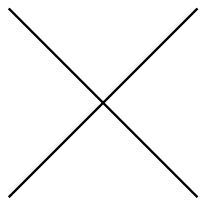


Figure 7: *Quartic vertex of exchanged gluons.*

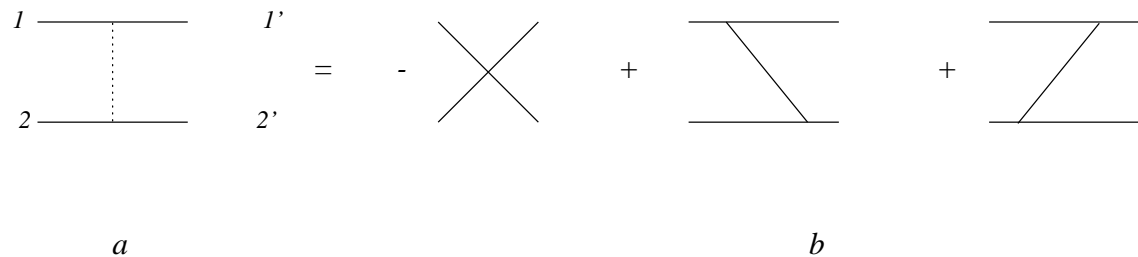


Figure 8: *The transition kernel  $2 \rightarrow 2$  in  $s$ -channel (a) and  $t$ -channel (b) representations.*

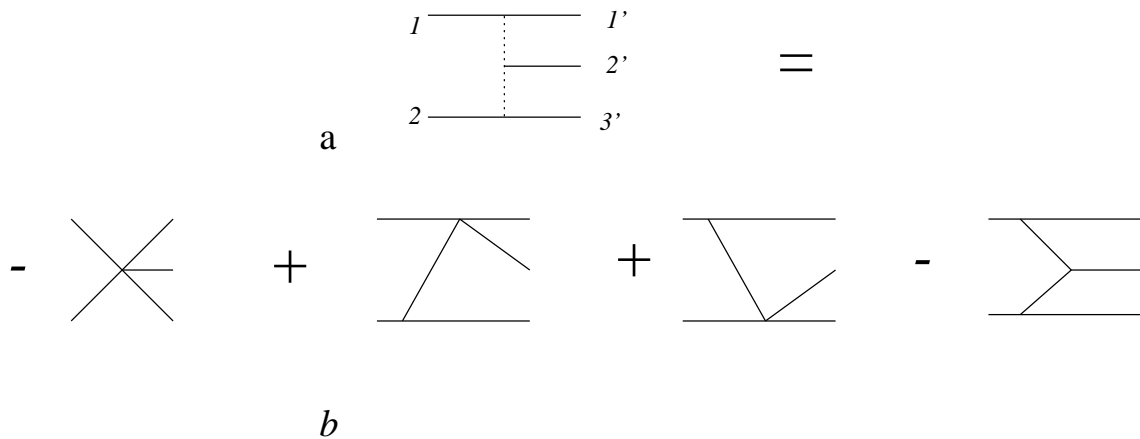


Figure 9: The transition kernel  $2 \rightarrow 3$  in  $s$ -channel (a) and  $t$ -channel (b) representations.

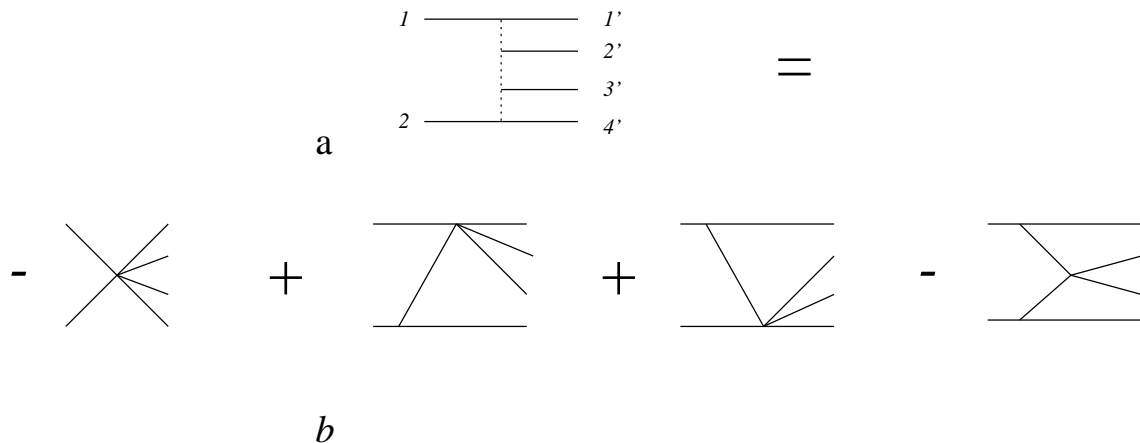


Figure 10: The transition kernel  $2 \rightarrow 4$  in  $s$ -channel (a) and  $t$ -channel (b) representations.

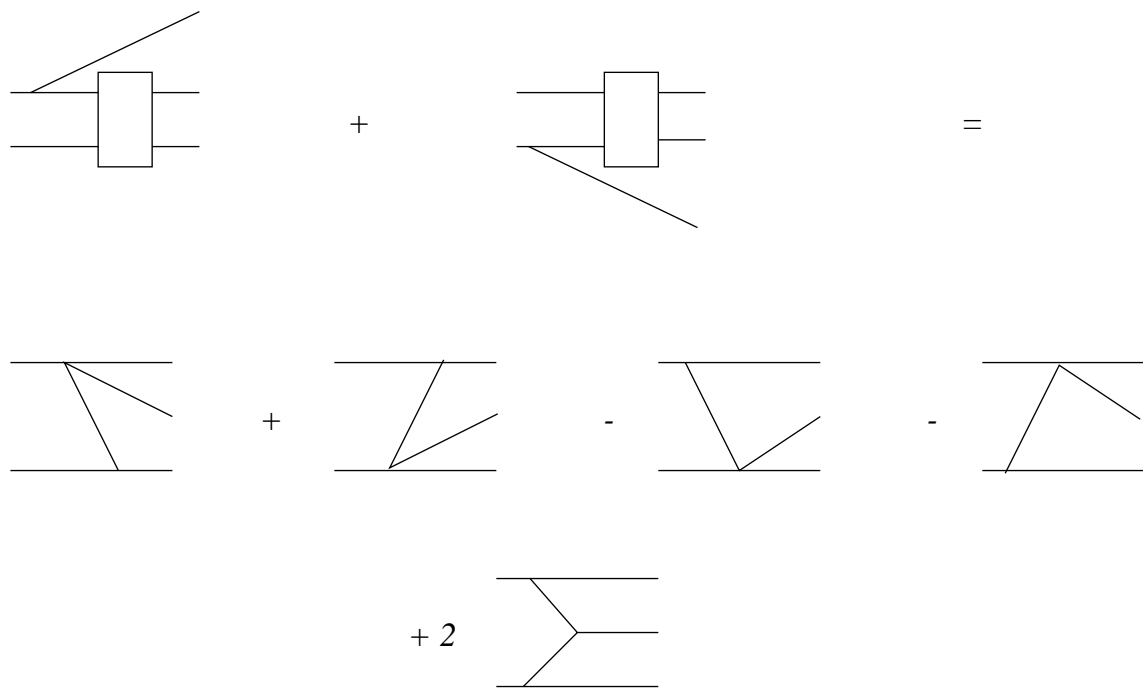


Figure 11: *Contraction of the  $2 \rightarrow 3$  splitting with the  $K_{2 \rightarrow 2}$  interaction.*

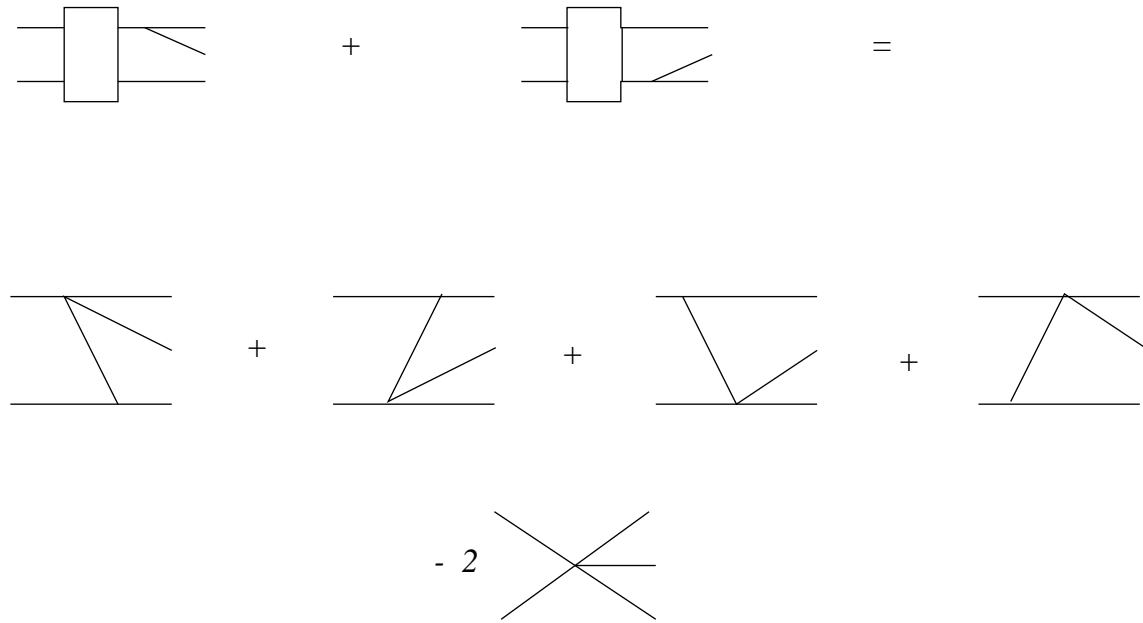


Figure 12: *Contraction of  $K_{2 \rightarrow 2}$  with the  $2 \rightarrow 3$  splitting.*

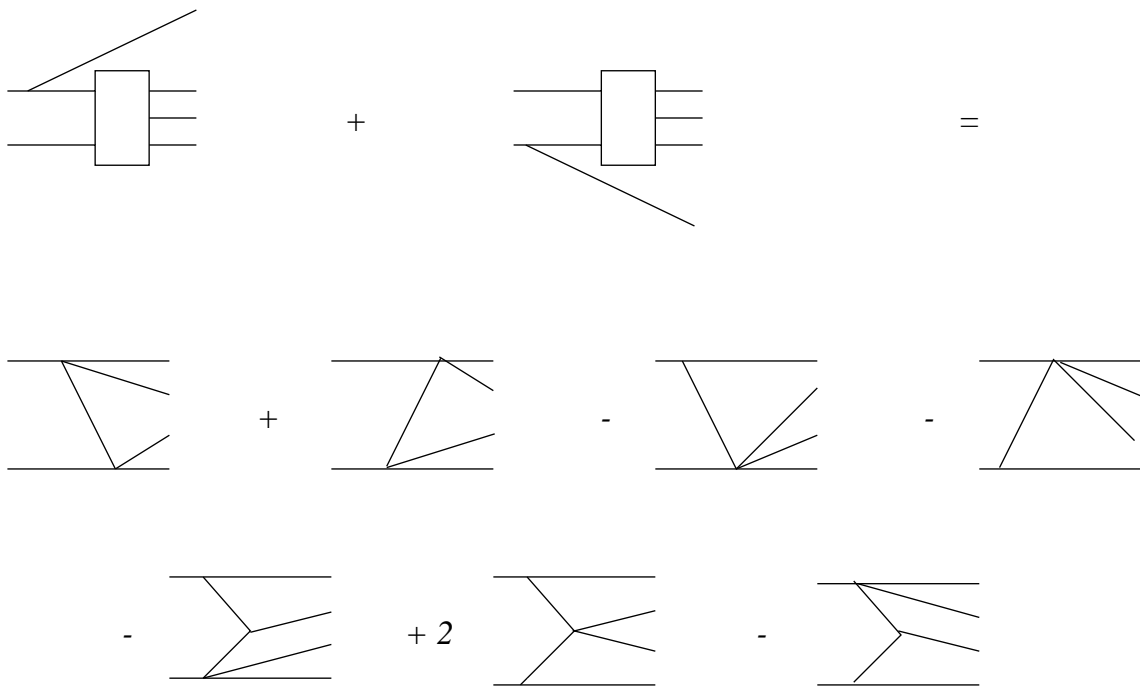


Figure 13: *Contraction of the  $2 \rightarrow 3$  splitting with the transition kernel  $K_{2 \rightarrow 3}$ .*

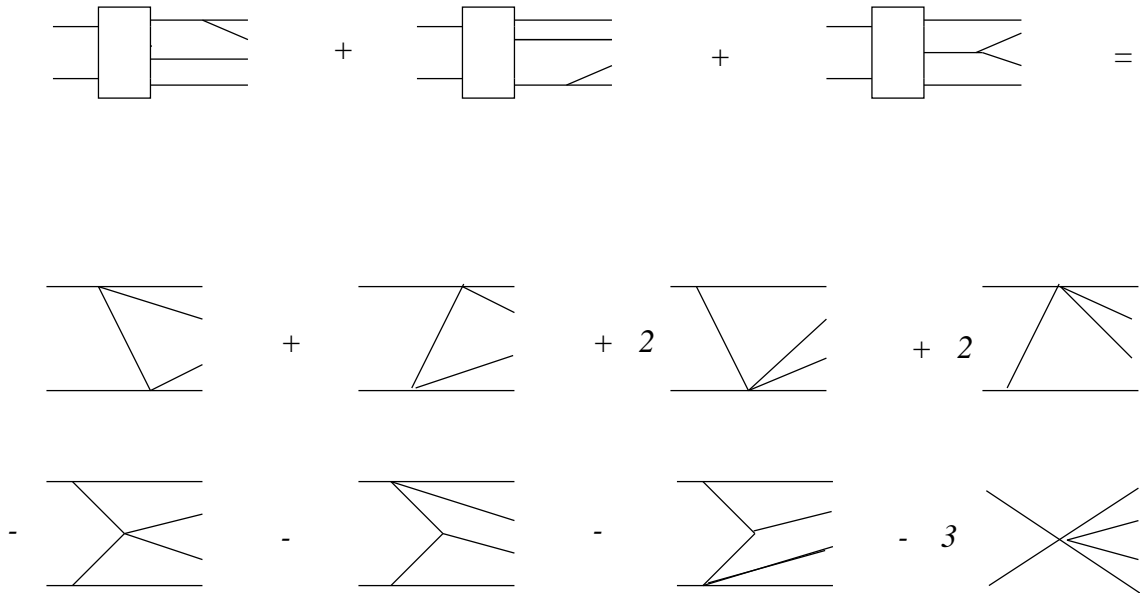


Figure 14: *Contraction of the transition kernel  $K_{2 \rightarrow 3}$  with the  $3 \rightarrow 4$  splitting.*

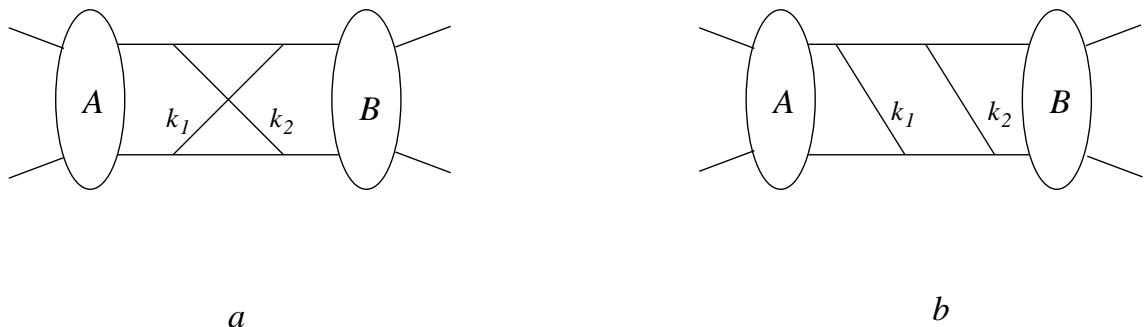


Figure 15: *Contributions to the scattering amplitude.*

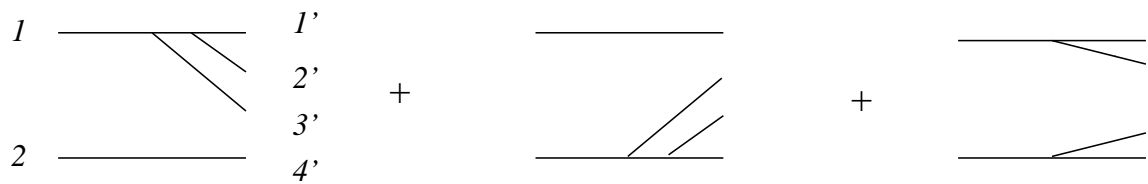


Figure 16: *Graphs contributing to the  $2 \rightarrow 4$  splitting.*

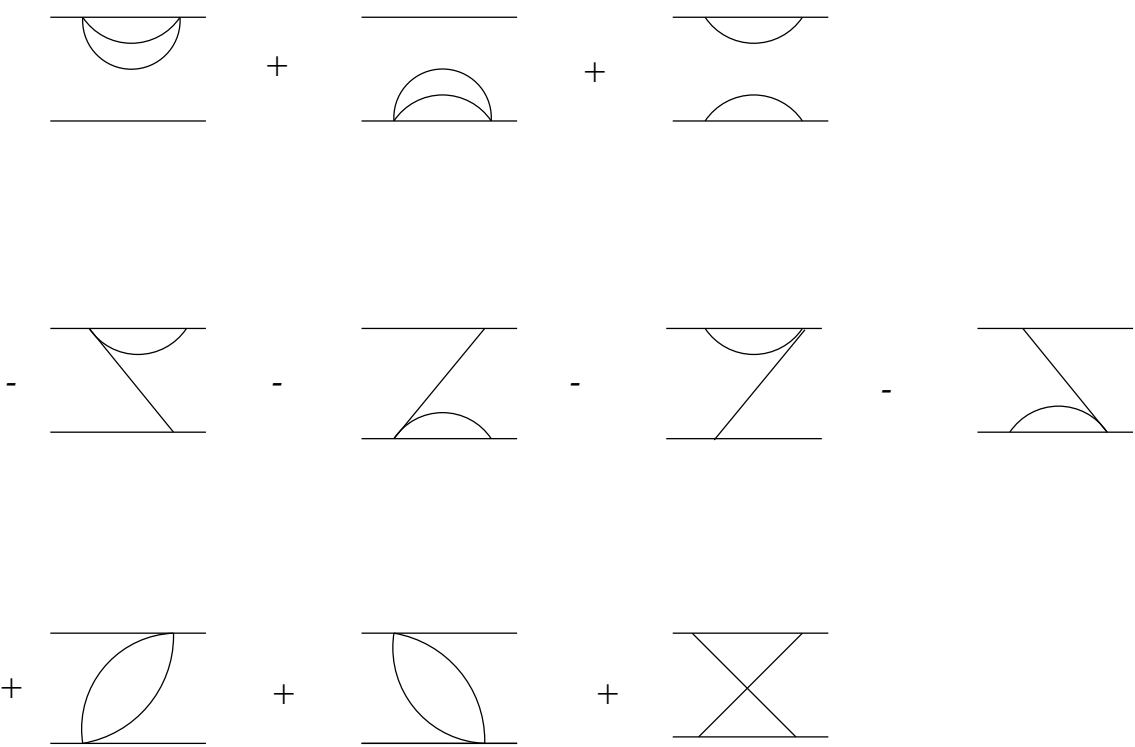


Figure 17: *Transverse momentum graphs for the one-loop correction to the  $2 \rightarrow 2$  reggeon Green function.*